In Situ Calorimetric Study of the Hexagonal-to-Lamellar Phase Transformation in a Nanostructured Silica/Surfactant Composite

Adam F. Gross,[†] Sanyuan Yang,[‡] Alexandra Navrotsky,*[,‡] and Sarah H. Tolbert*[,†]

Department of Chemistry and Biochemistry, University of California at Los Angeles, Los Angeles, California 90095-1569, and Thermochemistry Facility, Department of Chemical Engineering and Materials Science, University of California at Davis, Davis, California 95616

Received: August 27, 2002; In Final Form: January 22, 2003

Restructuring of hexagonal silica/surfactant composites under hydrothermal conditions was studied using in situ scanning microcalorimetry to understand the energetic changes associated with these rearrangements. Thermal processes can be associated with either changes in packing of the organic template or with chemistry of the cross-linked inorganic framework. To sort these out, calorimetric data were collected as composites were heated in water, where a hexagonal-to-lamellar phase transformation occurs, and as composites were heated in an acidic boric acid buffer, where no phase change is observed. The scanning calorimetric data were correlated with in situ low angle XRD to explore the relationship between rearrangements of the nanoscale architecture and the various energetic processes occurring in these materials. ^{29}Si NMR, which tracks changes in framework bonding, TGA and ^{1}H NMR, which measure surfactant loss from the composite, and ^{13}C NMR, which tells us about surfactant rearrangement and degradation, were also correlated with the calorimetric data. Both samples showed an endotherm at 70−71 °C that was assigned to an order−disorder transformation of the organic surfactant of the composite. In this same moderate temperature range, broad exotherms observed in both samples were associated with condensation of the silica framework. Two endotherms were observed in calorimetric scans of the water-treated composites that were not present in data collected on composites treated in boric acid. These endotherms were thus associated with the hexagonal-to-lamellar phase transformation, which has an enthalpy change of $+0.5 \pm 0.1$ kJ/(mol SiO_2) or $+2.4 \pm 0.3$ kJ/(mol surfactant) and entropy changes of $+1$ J K^{-1} (mol SiO_2)$^{-1}$ or $+6$ J K^{-1} (mol surfactant)$^{-1}$. The results quantify differences in thermodynamic stability in silica/surfactant composites and identify the physical, molecular, and nanoscale changes that influence stability in these materials.

Introduction

Phase transformations under hydrothermal conditions in periodic silica/surfactant composites provide an efficient way to synthesize new materials. These composites consist of organic domains with nanometer scale periodicities surrounded by a rigid, amorphous silica framework.[1] Some phases, such as the *p6mm* hexagonal phase or the lamellar phase, are easy to synthesize directly, but other phases, such as an *Ia*3*d* cubic phase or a *cmm* centered rectangular phase, are much easier to make through a phase transformation.[2−9] Understanding these transformations is thus important to be able to access novel and potentially useful nanostructures. While significant work has been performed to understand the molecular basis for activation barriers for these transformations,[3,5,6,10,11] little is known about the thermodynamics of the phase transition process.

In our previous studies on hexagonal-to-lamellar phase transitions in silica/surfactant composites, we have established that the silica framework acts as a kinetic barrier to the rearrangement of the periodic organic domains.[4,6,10,11] The solution pH during hydrothermal treatment strongly affects the height of the kinetic barrier because silica hydrolysis and condensation rates are very sensitive to pH.[11] Near neutral pH condensation is fast, but hydrolysis is very slow,[12] whereas the opposite is seen at high pH. As a result, composites hydrothermally treated at moderate pH have significantly higher activation energies for the hexagonal-to-lamellar phase transformation than those treated at high pH.[11] In fact, composites hydrothermally treated at pH 7 or 8 will not undergo a phase transition, whereas materials treated between pH 9 and 11 do rearrange. As the treatment pH decreases from 11 to 9, the activation energies increase, correlating with increasing silica condensation rates. Materials can be heated either isothermally using temperature jump techniques or under a linear temperature ramp to drive the phase transformation. Differences in temperature profiles do not affect the trends with pH and remarkably similar transformation activation energies are found with isothermal and nonisothermal methods.[11]

During hydrothermal heating of a silica/surfactant composite, both silica condensation and hydrolysis occur.[10] To date, changes in bonding have only been tracked using ex situ ^{29}Si MAS NMR, which provides data for just a few selected points during hydrothermal treatment. An in situ thermodynamic probe, such as scanning microcalorimetry, provides a different and continuous way to learn about bonding changes and the importance of various processes that evolve or require energy during hydrothermal treatment.[13] Scanning calorimetry is carried out in this work by heating an aqueous slurry of the composite and

* To whom correspondence should be addressed. E-mail: tolbert@chem.ucla.edu; anavrotsky@ucdavis.edu.

[†] Department of Chemistry and Biochemistry, University of California at Los Angeles.

[‡] Thermochemistry Facility, University of California at Davis.

10.1021/jp0268563 CCC: $25.00
Published on Web 02/27/2003

detecting the heat flow. To correlate the enthalpy changes with physical changes in the material, additional characterization techniques such as XRD and NMR are used. This combination of techniques has been successful in exploring chemical changes during zeolite formation and in monitoring the kinetics of zeolite crystallization.[13−17]

In these experiments, we heat a hexagonal silica/surfactant composite in both water and in an acidic boric acid buffer while performing scanning microcalorimetry to take advantage of pH control of silica chemistry. The composite in the boric acid solution will not transform to a lamellar phase because the material rapidly becomes too polymerized to rearrange. Thus, all calorimetric signals from this sample can be correlated with changes other than the hexagonal-to-lamellar transformation. By comparing data from samples treated in boric acid and in water (where a phase transition does occur), it is possible to identify the thermal signature of both pretransformation and transformation processes. We also correlate the calorimetric data with various other structural probes. In situ low angle XRD was employed to follow the phase transformation and thus to correlate heat flow with the rearrangement of the organic and inorganic domains during the hexagonal-to-lamellar phase change. ^{29}Si MAS NMR was performed to study changes in inorganic bonding. Finally, ^{13}C and ^{1}H NMR were performed to investigate changes in organic packing and to detect surfactant loss and degradation.

A number of processes likely to occur upon hydrothermal treatment should have calorimetric signatures. For example, silica hydrolysis is endothermic, whereas condensation is exothermic.[18,19] Tracking the absorption or release of heat during a hydrothermal process can thus constitute an in situ probe of changes in framework bonding. It appears that significant silica condensation occurs prior to the phase change, which can result in a more uniform hexagonal framework.[20−24] Scanning microcalorimetry can thus help identify condensation driven changes that occur in the hexagonal phase prior to the phase transformation.

The hexagonal-to-lamellar phase change is driven by changes in interfacial curvature caused by a change in the surfactant packing parameter.[6,25] When the surfactant is heated, the alkane tails becomes thermally excited and takes up more volume, effectively increasing the surfactant packing parameter.[26] This conformational disorder of the tails thus drives a rearrangement of the entire composite toward a structure with lower curvature, such as a lamellar phase. It has been shown that reorganization of alkylammonium surfactant micelles in solution has a detectable thermal signature,[27] and thus, it seems likely that increased tail disorder and repacking of the surfactant as a result of the hexagonal-to-lamellar phase transition will be observable in these calorimetric experiments.

Hydrothermal restructuring in silica surfactant composites is complicated by the fact that surfactant expelled into the hydrothermally solution can undergo Hoffman degradation to form a tertiary amine.[28−32] Once the amine is formed, it can re-enter the organic domains of the surfactant to escape the hydrophilic water environment. The degradation of the amine will have a heat of reaction associated with it that may be possible to detect. In addition, when the amine leaves the hydrophilic water environment and enters the hydrophobic surfactant tail areas, this will change the solvation energy of the amine.[33,34] This change may also have a detectable thermal signature.

The overall goal of these experiments is thus to identify the relative energetic importance of each of the processes that occur during hydrothermal rearrangements and phase transformation. This information will provide better understanding of how a phase transformation in inorganic/organic composites occurs, which may make it easier for a synthetic chemist to drive a desirable phase transformation during the assembly of a novel composite material. Finally, this work assesses the applicability of in situ scanning microcalorimetry for learning about structural rearrangements in complex inorganic/organic composite materials.

Experimental Section

The synthesis of the silica/surfactant composites used in this work has been described in depth previously.[2,10] Briefly, samples were synthesized using tetraethyl orthosilicate (TEOS), an eicosyltrimethylammonium bromide surfactant (ETAB), and aqueous sodium hydroxide (with a final concentration of 0.235 M). After isolation and drying, samples were mixed with water or a 0.250 M boric acid buffer and heated under hydrothermal conditions. The boric acid buffer was created by mixing a solution of pure boric acid (pH $<$ 5) with the composite. Residual base on the composite reacts with the acid to create a buffer with pH $\sim$ 6.4. After hydrothermal treatment, this value climbs to pH $\sim$ 7.2.[20] Boric acid was chosen instead of other acids because the electron deficient nature of the borate anion appeared to minimize undesirable chemistry between the anion and the quaternary ammonium surfactant. In water, a hexagonal-to-lamellar transformation occurred, whereas no phase change was observed with the boric acid solution.[11]

Four batches of composite synthesized separately were mixed together and subsequently used for all calorimetry experiments. The composite was mixed in a 1:7 mass:mass ratio with water or a boric acid solution and heated at 0.25 °C/min in a Setaram C-80 Calvet-type differential heat flow calorimeter.[13] The hydrothermal mixture was sealed in a Hastelloy-X vessel. A mass of water or boric acid with heat capacity similar to the silica and solution in the sample vessel was sealed in another vessel and used as a reference. The reference reduced the baseline offset of the scanning calorimetric heat flow. To minimize heat effects coming from heating the solution and selectively observe heat effects from changes in the composite, a baseline curve was further subtracted from the original scanning calorimetric heat flow. The baseline was obtained by heating the sample a second time after all rearrangements were complete. This methodology is similar to that used recently for the study of a zeolite synthesis.[17]

Structural changes were followed using real time X-ray powder diffraction. Data were collected by heating a slurry of the composite and water or boric acid solution under a linear temperature ramp of 0.25 °C/min. In situ low angle scattering was collected using Kα Mo radiation from a Rigaku UltraX 18 rotating anode X-ray generator; a Roper Scientific X-ray CCD camera was used to acquire a diffraction pattern every five minutes during heating to follow structural changes with time. The details of the experimental setup have been presented elsewhere.[6,10,35] X-ray diffraction patterns were fit to Gaussian functions to find peak areas and positions.

Composites were characterized by ^{29}Si and ^{13}C MAS NMR using a Bruker Avance 300 spectrometer. ^{29}Si spectra were collected using a standard one-pulse acquisition with a 240 s recycle delay, whereas ^{13}C MAS-NMR spectra were collected using high power proton decoupling during a standard one-pulse sequence. Samples used for NMR spectroscopy were used as-synthesized or were hydrothermally treated in sealed ampules in a 0.25 °C/min temperature ramped oil bath. At various

temperatures, samples were removed from the bath, rapidly quenched to room temperature, and filtered for NMR analysis as dry powders. Tetrakis-(trimethylsilyl)silane was used as a reference for both silicon (0 ppm) and carbon (3.50 ppm).[36]

The amount of surfactant expelled from the composite during heating was analyzed using ^{1}H NMR on a Bruker ARX 500 spectrometer and a Perkin-Elmer TGA 2950 thermogravimetric analyzer. Samples for NMR were made by collecting the supernatant from the oil bath heating experiments described above and mixing these solutions with a standard [trimethysilylpropionic acid (2,2,3,3 deuterated)] dissolved in methanol. Surfactant concentrations were determined by comparing the triplet from the $-CH_3$ at the end of the surfactant alkane tail ($\sim$0.8 ppm) with the single standard peak (~ -0.1 ppm). TGA was also performed on a portion of the samples used for ^{29}Si NMR. These samples were heated at a ramp rate of 10 °C/min under flowing dry compressed air to 800 °C to find the mass loss. The change in mass was assumed to stem from combustion of the organic and loss of water from silica condensation. The change in silica polymerization upon heating was quantified using ^{29}Si MAS NMR, which then allowed the organic content of each sample to be calculated from the TGA weight loss.

Changes in surfactant packing in the pores were followed using ^{13}C NMR with a 20 mm broadband liquid probe in a Bruker Avance 300 NMR spectrometer. Proton decoupled spectra were collected as the sample was heated in $\sim$10 °C steps. The exact temperature was calibrated using the temperature dependent chemical shift of ethylene glycol.

Results and Discussion

1. Nanoscale Changes in Periodicity during Hydrothermal Heating. When heated in water, a silica/surfactant composite will undergo a hexagonal-to-lamellar phase transformation as shown in Figure 1, top. At the start of the 0.25 °C/min heating ramp, four diffraction peaks that can be indexed to a *p6mm* two-dimensional hexagonal phase are observed. As a result of composite restructuring, the hexagonal peaks first grow in intensity and then lose intensity as two evenly spaced peaks that can be indexed to a lamellar phase appear. The smallest height of the fundamental diffraction peak is seen when approximately equal amounts of both phases are present. The lamellar peaks grow with increasing temperature until only the lamellar phase is present. This change is not observed for a composite heated in a boric acid buffer (Figure 1, bottom). Throughout the ramp, the four hexagonal peaks are always present. Previous work has shown that the very well condensed silica framework resulting from boric acid treatment is unable to rearrange.[11,20] In this work, we compare the scanning calorimetric signals obtained under transforming (water) and nontransforming (boric acid) conditions to learn about the energetic processes that occur during a phase transition in silica/surfactant composites.

2. In Situ Scanning Calorimetry. The background subtracted scanning calorimetric heat flow curves for composites heated in water and boric acid are shown in Figure 2. The data do not start until 50 °C because the background in the second heating cycle shows a large endotherm at lower temperature. This endotherm results from surfactant loss from the composite into solution. This free surfactant precipitates as the vessel is cooled after the first heating, and redissolution produces a peak in the background data. Above 50 °C, the scanning calorimetric heat flow curves from both water and boric acid treated samples show a sharp endotherm at 70−71 °C and look nearly identical until approximately 110 °C. The data for the water-treated sample

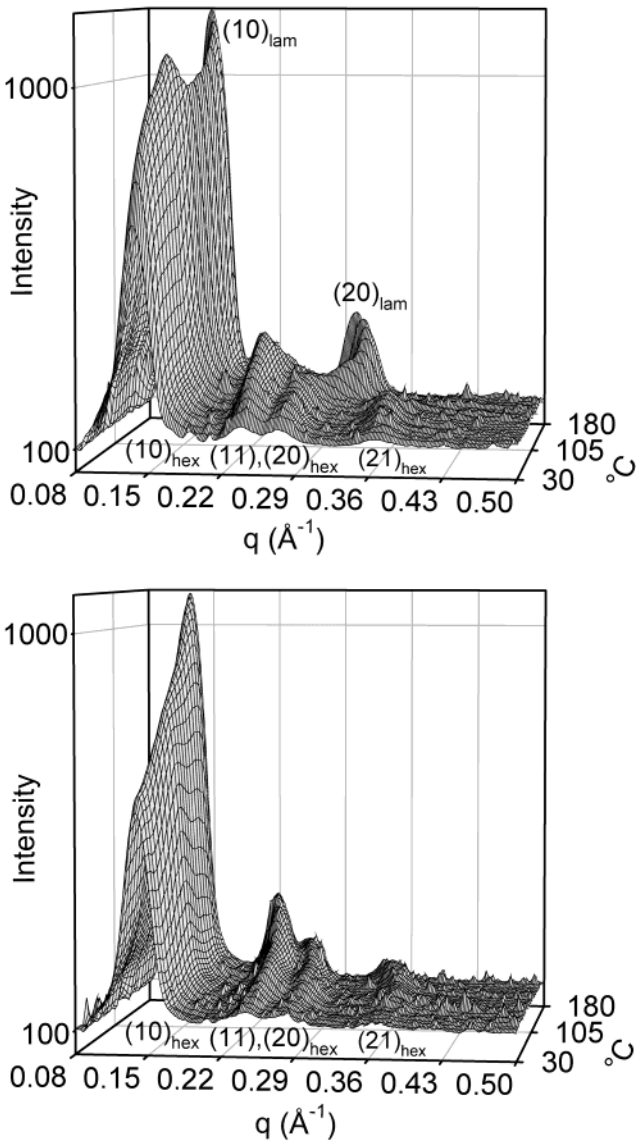

Figure 1. Low angle X-ray diffraction data collected on hexagonal silica/surfactant composites heated at 0.25 °C/min in water (top) or a boric acid buffer (bottom). Diffraction peaks are indexed on each graph. Only the sample treated in water (top) transforms from a 4-peak hexagonal pattern to a 2-peak lamellar pattern. The boric acid treated sample remains in the hexagonal phase throughout the heating ramp. For both samples, the diffraction peaks shift to lower *q* at very high temperature, indicating expansion of the nanoscale structure.

are endothermic above 110 °C and show two endothermic peaks between 110 and 160 °C. The curve then shifts farther in the endothermic direction relative to the reference above 160 °C. By contrast, the data for the boric acid treated composite show much less pronounced thermal effects between 110 and 160 °C and then shift in an exothermic direction above 160 °C.

3. Silica Polymerization and the 50−110 °C Exothermic Region. The Q^4/Q^3 peak area ratio from ^{29}Si NMR is shown versus temperature for a composite heated in water in Figure 3, top. The Q^4 peaks arise from Si bonded to four other Si atoms through oxygen bridges and indicate a fully condensed silica structure. The Q^3 peak indicates Si with three Si−O−Si linkages and one terminal Si−O$^-$ or Si−OH group; Q^3 Si is either a defect or part of the very large interfacial area always present in these materials. A sample is most polymerized when it has the largest Q^4/Q^3 peak area ratio. The increase in Q^4/Q^3 peak area ratio up to $\sim$90 °C for a composite hydrothermally heated in water (Figure 3, top) results from condensation. Because silica

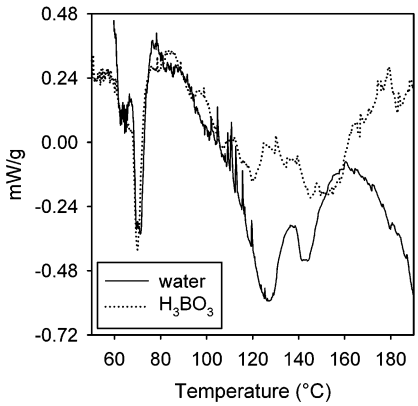

Figure 2. Scanning calorimetric heat flow for a silica/surfactant composite hydrothermally heated in water (solid line) or in a boric acid buffer (dotted line) at 0.25 °C/min. Positive values correspond to exothermic heat flow. The water-heated sample undergoes a hexagonal-to-lamellar phase transformation, whereas the boric acid heated sample remains in the hexagonal phase throughout the heating ramp. The two samples are nearly identical at low temperature (up to ∼110 °C), but two endotherms are present in the water data in the vicinity of the phase transition that are not observed for the boric acid treated material.

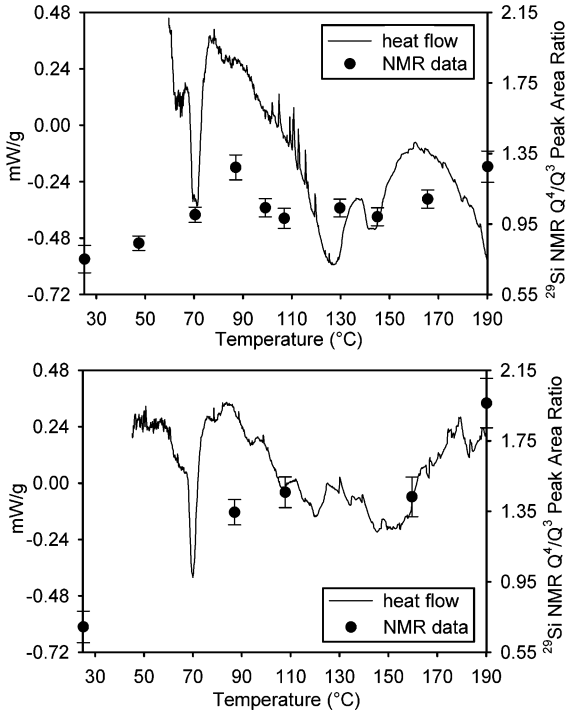

Figure 3. Change in silica polymerization obtained from ^{29}Si MAS NMR and scanning calorimetric heat flow versus temperature for composites hydrothermally heated in water (top) or in a boric acid buffer (bottom). A larger Q^4/Q^3 ratio indicates a more condensed composite. Silica condensation is an exothermic process, whereas hydrolysis is endothermic. For temperatures up to 90 °C (top) and 110 °C (bottom), exothermic regions of the scanning calorimetric heat flow correlate with an increase in the Q^4/Q^3 ratio.

polymerization is exothermic, it is reasonable to observe an exothermic region in the calorimetric data up to ∼90 °C. Endothermic hydrolysis begins above ∼90 °C as shown by the drop in the Q^4/Q^3 ratio. This correlates well with the crossover from exothermic to endothermic behavior in the scanning calorimetric heat flow curve between 100 and 110 °C. Silica condensation is also found to coincide with exothermic behavior in the boric acid treated sample (Figure 3, bottom). An increase in polymerization is seen up to 110 °C. In this case, however, little hydrolysis (or drop in the Q^4/Q^3 ratio) is observed above 100 °C, and the scanning calorimetric heat flow curve does not show a crossover to significantly endothermic behavior relative to the reference.

Using the boric acid calorimetric data (Figure 2) and the change in silica polymerization from Figure 3, bottom, we find that the change in enthalpy to make an Si−O−Si linkage from 2 Q^3 silica species is −2.7 kJ/(mol Si−O−Si bonds).[37] This number is reasonable in light of the enthalpy change to fully dissolve silica, which is 15.5 kJ/(mol SiO_2).[18] One-quarter of the total hydrolysis enthalpy, or 3.9 kJ/(mole bonds), is a very rough approximation of the energy to break just one Si−O−Si bond. Because hydrolysis and condensation are reverse reactions, it is reasonable that these values should be close in magnitude, but opposite in sign.

4. Surfactant Rearrangement and the 70 °C Endotherm. The endotherm at 70−71 °C appears to be almost identical for both the water and boric acid treated samples. The hydrothermal treatment conditions result in approximately the same framework condensation in the two samples (Figure 3, top and bottom) up to 90 °C, so it is possible that the endotherm is caused by hydrothermal silica chemistry. However, when a dry composite is heated in the calorimeter, this peak is also observed, although the temperature is ∼3 °C higher. This suggests that this endothermic peak does not result from hydrothermal silica chemistry or from reactions in solution. More evidence that the sharp endotherm is not caused by silica chemistry is shown in Figure 3, top. There is a monotonic increase in silica polymerization from 25 to 87 °C, and no deviation from this trend is observed around 70 °C, thus arguing against a sharp change in hydrolysis at 70 °C.

A more likely cause for this endotherm is the rearrangement of surfactant in the organic domains of the composite. NMR can be used to investigate changes in the structure of mobile organic groups. For example, it is known that the packing of chains of polymers affects the chemical shifts of all peaks.[38] The same effect occurs in surfactants; a change in ^{13}C NMR peak positions may be correlated with a change in surfactant packing.[39,40] The main tail peak shifts downfield when the tail takes on more of an all trans configuration like that in crystalline surfactant.[39] Heating a surfactant micelle solution has the opposite effect; an increase in temperature causes an upfield shift. Other structural changes can also be detected with NMR: during a glass transition in polymer blends, the widths of ^{13}C lines broaden significantly. This results from a distribution of chemical shifts caused by a variety of local conformations of the polymer.[41] Thus, by observing NMR peak positions and widths, it may be possible to understand if a change in surfactant domain morphology occurs at 70 °C.

To study changes in tail structure, the composite was mixed with water and ^{13}C proton decoupled NMR spectra were collected at various temperatures. NMR spectra of composite heated in water are shown in Figure 4, top. The spectra look similar from 29 to 63 °C, but at 71 °C, a broadened and slightly shifted spectrum is seen. At 79 °C, an upfield shifted spectrum with a much narrower main alkyl tail peak is observed. Figure 4, bottom, shows changes in peak position and width for the main surfactant alkyl tail peak (observed at ∼29 ppm). The peak moves downfield up to 71 °C, suggesting that the surfactant tails are increasingly taking on an all-trans configuration as the sample is heated. As the temperature is raised to 79 °C, however, the surfactant tails appear to randomize, as evidenced by the sharp upfield shift in peak position, producing a spectrum that is similar to surfactant micelles in solution. The sudden change in NMR peak position and the upfield peak position that results

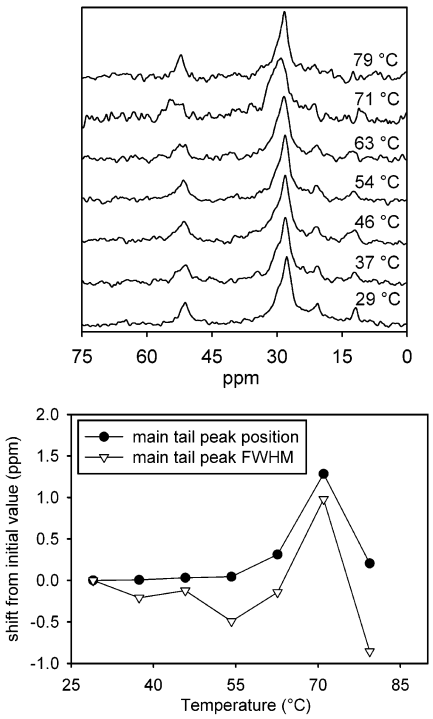

Figure 4. (Top) In situ ^{13}C NMR spectra of a slurry of composite and water heated to various temperatures (shown on graph). The spectra look similar up to 71 °C, at which point the surfactant alkyl tail peak (29 ppm) broadens and shifts. (Bottom) Change in peak position and fwhm for the surfactant tail peak (observed at 28−30 ppm). The shift in the fwhm is indicative of a melting transition, whereas the shift in the surfactant tail peak position indicates a change in surfactant tail conformation.

suggests that an order−disorder rearrangement of the surfactant tails occurs at or slightly above 71 °C. Figure 4, bottom, also shows significant broadening of the main tail peak of the NMR spectra at 71 °C, which could result from site inhomogeneity during the order−disorder transition. At higher temperatures, however, motional narrowing in the melted, micelle-like surfactant tails produces significant peak narrowing. Changes of this sort have been observed at the glass transition for polymer blends.[41] On the basis of the shift in peak position and broadening of the main tail peaks at 71 °C, we thus assign the endotherm near 70 °C in Figure 2 to a reorganization of surfactant in the organic domains of the composite, specifically a tail melting transition.

5. Scanning Calorimetric Heat Flow from 110 to 160 °C. From 110 to 160 °C, the sample hydrothermally treated in water undergoes a hexagonal to lamellar phase transition and the scanning calorimetric heat flow shows two distinct endotherms. Figure 5 plots the $(10)_{hexagonal}$ peak area from XRD (shown in Figure 1, top) overlapped with the scanning calorimetric heat flow curve. The drop in the $(10)_{hexagonal}$ peak area indicates transformation of the composite to a lamellar phase; when no $(10)_{hexagonal}$ peak is left, the transformation is complete. The two endotherms from 110 to 160 °C roughly overlap the change in the XRD $(10)_{hexagonal}$ peak area. Conversely, in a boric acid treated sample, which remains hexagonal, endothermic behavior is not observed between 110 and 160 °C. We thus associate these endotherms with the phase transition process; the question now is to establish the molecular basis for this behavior.

The 110−160 °C endotherms in the water-treated sample could result from changes in the inorganic or organic domains of the composite or from reactions in the aqueous solution. Some endothermic silica hydrolysis is expected in order to facilitate

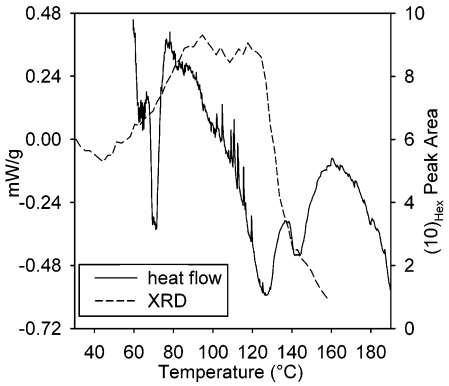

Figure 5. Integrated area of the hexagonal (10) diffraction peak (dashed line) and scanning calorimetry heat flow (solid line) as a function of temperature for a composite heated at 0.25 °C/min in water. The hexagonal phase peak area falls as the material undergoes a hexagonal-to-lamellar phase change. The phase transformation occurs over the temperature range where the two endotherms from 110 to 160 °C are seen in the scanning calorimetric heat flow curve, suggesting that these endotherms correspond to the rearrangement process.

the phase transformation process,[10] and in agreement with this, a clear decrease in Q^4/Q^3 ratio is observed between 90 and 110 °C. Framework polymerization data for a sample heated in water (Figure 3, top), however, shows negligible change in silica polymerization from 110 to 160 °C. It thus appears that silica hydrolysis and the accompanying endothermic behavior is a pretransformation process that is virtually complete by 110 °C.

5.A. Changes in Chemical Composition. Hydrothermal treatment and phase transitions can also cause changes in the overall composition of the composite, and such changes could have a significant calorimetric signal. When a surface $Si-O^-$ species that is electrostatically bound to a surfactant condenses with another Q^3 species to form two Q^4 species, an OH^- ion may be liberated. If this hydroxide ion diffuses away, the surfactant that was bound to the Q^3 site may also diffuse into solution. Once surfactant leaves the organic domain, reactions may occur in solution. Figure 6 shows the fraction of total surfactant found in solution as a function of temperatures. Data were collected by running ^1H NMR on the hydrothermal solution or by using TGA analysis of a hydrothermally treated composite to track the total amount of organic in the composite at different temperatures. The NMR shows more surfactant in solution than TGA at 25 °C because, when the composite is mixed with water, some surfactant is washed into solution at 25 °C. The 25 °C TGA sample was not mixed with water to wash away this excess surfactant. At higher temperatures, the data from TGA and NMR agree very well.

The amount of surfactant in solution from a water-treated composite increases until 100 °C and then decreases until essentially no surfactant is found in solution at 190 °C. The overall decrease of soluble organic probably results because surfactant in solution can degrade into a tertiary amine (dimethyleicosylamine) that subsequently re-enters the organic domain in the composite to escape from the hydrophilic water environment.[28−32] We can confirm that the amine reenters the organic regions in two ways. The first evidence is the fact that we see a decrease in the amount of organic in solution by both NMR and TGA as the temperature increases from 100 to 190 °C. Both the amine and surfactant show identical 0.8 ppm terminal methyl peaks; thus, we should see both organic molecules in solution using NMR spectroscopy. TGA, which does not discriminate between types of organics, also shows more organic material present in the composite as the temperature increases from 100 to 190 °C. The second piece of

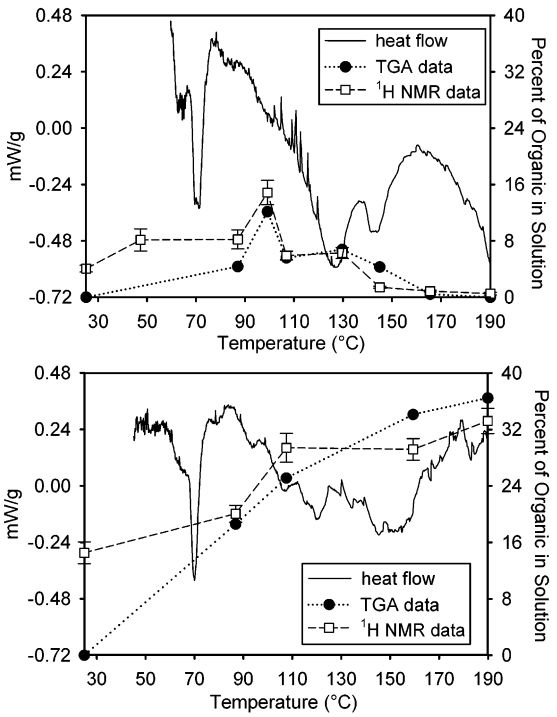

Figure 6. Fraction of the total organic in the silica/surfactant composite that is lost into solution during hydrothermal treatment in water (top) or in a boric acid solution (bottom) as a function of temperature. Organic loss was found using ^{1}H NMR and TGA. The NMR data starts at a nonzero value because surfactant is washed into solution immediately upon mixing with water. Legends are on both graphs, and the data are overlaid with the scanning calorimetric heat flow curves. Treatment in water causes a loss of surfactant up to 100 °C. This surfactant then degrades into a tertiary amine and re-enters the organic domains of the composite. By contrast, boric acid treatment produces steadily increasing amounts of surfactant in solution with increasing temperature.

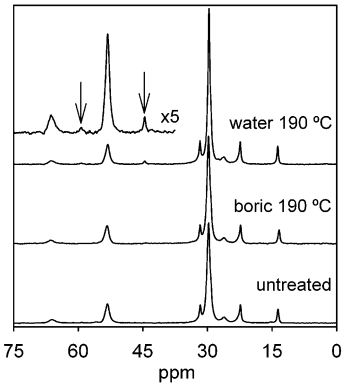

Figure 7. ^{13}C MAS-NMR spectra of an untreated composite (bottom), a composite hydrothermally treated to 190 °C in boric acid (middle), and a composite hydrothermally treated to 190 °C in water (top). Peaks from the surfactant degradation product, dimethyleicosylamine, are not visible for an untreated sample but can be clearly seen in the spectra from the sample hydrothermally treated to 190 °C in water. The amine peaks at 45.6 and 60.1 ppm are indicated on the enlargement of the spectra with arrows and correspond to 11% of the surfactant in the composite in the form of the neutral amine. There is also a small amount of amine (3%) in the boric acid treated sample.

evidence supporting the idea that amine enters the pores is the direct observation of amine in hydrothermally treated composites using solid-state ^{13}C MAS NMR. Figure 7 (top trace) displays ^{13}C MAS NMR performed on a composite hydrothermally treated to 190 °C in water. The spectrum clearly shows peaks from the two methyl groups on the amine (45.6 ppm) and from the α carbon on the amine alkyl chain (60.1 ppm). Integration of the amine NMR peaks indicate that 11% of the organic in the composite is the amine. This value agrees reasonably well with the change in solution phase surfactant concentration observed between 100 °C and 190 °C shown in Figure 6, top. The amine NMR peaks do not exist in the spectrum taken on untreated composite (Figure 7, bottom), showing that the amine enters the composite during hydrothermal treatment and not during synthesis.

5.B. Calorimetric Signatures from Changes in Chemical Composition. A series of experiments were performed to determine if surfactant degradation to form an amine or reincorporation of the amine into the composite could be responsible for the broad endotherms observed between 110 and 160 °C for samples treated in water. By heating a 1% by mass solution of surfactant in a basic buffer (to catalyze degradation), it was found that the degradation of hydrothermally heated surfactant is exothermic. Thus, surfactant degradation cannot be the cause of the endotherms from 110 to 160 °C.

The amine also reenters the organic domains in the temperature range between 110 and 160 °C. To learn about the thermal flux from the amine entering the composite, a calorimetry experiment was performed in which dimethyloctadecylamine was injected into a mixture of lamellar composite, surfactant, and water at 25 °C. When the amine is injected into a surfactant and water solution with no composite present, a very small exothermic signal is observed. With the composite in the solution, almost an order of magnitude increase in the exothermic signal was detected, associated with amine entering the pores. The difference of these two calorimetric experiments gives the molar heat associated with amine entering the organic region. It is necessary to take this difference to correct for the heat of mixing of the amine with water in the hydrothermal solution. For dimethyloctadecylamine entering the organic domains of a lamellar composite, the process is exothermic with an enthalpy change of −3 mJ/(g composite) when performed with an amine concentration of 0.015 M. Although the amine concentration and thus the enthalpy change is likely to be significantly lower for our composite samples, the fact remains that the scanning calorimetric heat flow in Figure 2 is endothermic from 130 to 166 °C, where most of the amine enters the organic regions of a composite (Figure 6, top). It thus appears that changes in composite composition during the phase transition cannot explain the endothermic region between 110 and 160 °C in Figure 2.

5.C. Silica Hydrolysis During the Phase Transition. The results presented above lead us to the conclusion that that the atomic and molecular rearrangements of the phase transformation itself must be responsible for the endothermic behavior. Evidence for this idea can be found in a closer examination of Figure 5. The first endothermic peak correlates well with the main hexagonal-to-lamellar rearrangement above 120 °C where the $(10)_{hexagonal}$ XRD peak area first drops. Looking closely at the $(10)_{hexagonal}$ XRD peak area in Figure 5, however, we note that the hexagonal phase peak area shows two distinct slopes as it decreases, suggesting that the transformation proceeds in two stages. The second, more gradual stage correlates well with the second endothermic peak observed around 140 °C.

We can understand why a transformation might proceed in stages by considering how hydrolysis, which is necessary for the phase transformation to progress, is correlated with strain in the silica network.[10,11] In bulk silica, theoretical calculations have shown that the activation energy for single hydrolysis events decreases with increased strain in the silica network.[42] If hydrolysis occurs at a very strained site, the activation energy is on the order of 9.6−29 kJ/(mol Si−O−Si bonds), and the

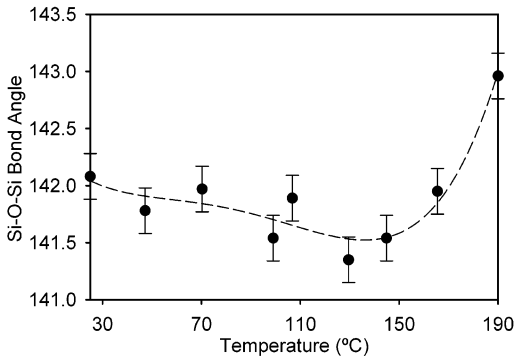

Figure 8. Si-O−Si bond angles calculated from ^{29}Si MAS-NMR data versus temperature for a sample heated in water at 0.25 °C/min. The dashed line is a 4th order polynomial fit to the data and is intended only to guide the eye. The equilibrium bond angle found in vitreous silica is 144°; as the bond angle deviates from this value, more strain is built into the network. From the data, strain increases in the framework during low temperature hydrothermal processing but stays virtually constant during the hexagonal-to-lamellar phase transition. The lamellar phase initially formed in the phase transition process thus appears at least as strained as the hexagonal phase. This strain relaxes, however, as the material is hydrothermal treated to higher temperatures.

reaction can even be exothermic.[43] If the network is unstrained, the barrier can be as high as 154 kJ/(mol Si−O−Si bonds), and the reaction is endothermic by as much as 68 kJ/(mol Si−O−Si bonds), as expected for silica.[43] We know there is strained silica in the framework because we can calculate the energy per bond broken by integrating the calorimetric heat flow from 87 to 107 °C and dividing by the number of bonds broken over this temperature range using ^{29}Si NMR data (Figure 3, top). This temperature range is chosen because the sample is in the hexagonal phase throughout this region. We find that each bond breaking has a very small reaction energy change of 1.6 kJ/(mol Si−O−Si bonds broken), suggesting a very strained silica network at the start of the transformation.

^{29}Si MAS-NMR data support the idea of a strained silica network in the composites during the phase transition. It is possible to find the average Si−O−Si bond angle using the Q^4 ^{29}Si MAS-NMR peak.[44] Vitreous silica has an average Si−O−Si bond angle of 144°; as the bond angle becomes higher or lower than 144°, more strain is present in the framework.[44] Figure 8 shows the average Si−O−Si bond angle as a function of temperature for a composite heated in water. The average bond angle starts out at 142° and then decreases further, indicating an increasing amount of strain in the silica framework as the composite is heated to ∼100 °C. It then stays nearly constant up to 147 °C (through the first part of the phase transition). Finally, an increase in bond angle toward the equilibrium value of 144° and a decrease in strain with increasing temperature occur at high temperature. The increase of strain as a result of hydrothermal treatment at low-temperature lowers the kinetic barrier to transformation and may be necessary to allow the hexagonal-to-lamellar phase change to occur.

We thus propose that the endotherm in the scanning calorimetric heat flow between 120 and 140 °C results from a hexagonal-to-lamellar transformation in composite with a strained silica framework. Once the transformation has proceeded, the remaining hexagonal structure may be more relaxed. As a result, higher temperatures are needed to drive the reaction to completion, resulting in the second endotherm in the scanning calorimetric heat flow from 140 to 160 °C and the flatter slope in the $(10)_{hexagonal}$ area loss in Figure 5. We note that a significant increase in the Si−O−Si bong angle is not observed at the phase transition point, suggesting that the as-formed lamellar phase is also quite strained. If these ideas are correct, rearrangements occurring in the 140−160 °C region should be more endothermic than transformations that occur at lower temperatures, because the initial phase is more relaxed. In agreement with this, only 25% of the composite transforms in the second, higher temperature step (Figure 5, peak area ∝ population). By contrast, the second endothermic peak is about 40% the total area between 120 and 160 °C, indicating that a larger enthalpy change is associated with this second process.

5.D. Thermodynamic Consequences. The fact that the hexagonal-to-lamellar phase transformation is endothermic implies that rearrangements in silica/surfactant composites are entropically driven and may be near-equilibrium transitions. Reversible transformations that occur upon an increase in temperature must involve an increase in entropy and thus must be endothermic.[45−47] By contrast, if the transition was highly irreversibly because the low temperature phase was energetically metastable at the transition temperature, an exothermic enthalpy of transformation would be expected, which is not observed.[48] The positive enthalpy of transformation thus implies that the hexagonal phase is thermodynamically stable at low temperature and the lamellar phase is stable at high temperature. The phase transformation could result from the increased accessibility of states in the lamellar phase, which is probably related to increased conformational disorder of the surfactant tails in the unconfined lamellar structure. Thus, although these transitions are not experimentally kinetically reversible, the calorimetric data suggest that the transition could be nearly thermodynamically reversible with the equilibrium temperature of the phase change only slightly below the observed transformation temperature.

It is interesting to note that, in most atomically ordered materials, temperature induced phase transitions involve transitions from a lower symmetry phase at low temperature to a higher symmetry phases with more equivalent positions at high temperature.[45,46,47] Because our system is periodic, but not crystalline, however, we see very different behavior. Our high temperature lamellar phase is lower symmetry than the low temperature hexagonal phase, and in fact these phases have opposite group/subgroup relationship to those normally observed in crystalline solids. Because atomic scale disorder is not coupled by symmetry to the nanoscale periodicity in these inorganic/organic composite materials, we find that the lowest symmetry, least constrained phases have the higher entropy. This observation sheds some light on the notoriously difficult synthesis of the *Ia3d* cubic structure, which is often formed at high temperature through a phase transition process.[3−5,7,8,49] The difficulty of the synthesis has frequently been explained using kinetic arguments, but thermodynamics may also play a role.[4,5] The *Ia3d* cubic structure is a very high symmetry phase and thus should produce a more confined environment for the surfactant. As a result, this phase should be less favored entropically and thus should require a large enthalpic driving force for formation. In agreement with this idea, it is easier to form the cubic phase at room temperature with a designer surfactant that has the appropriate curvature.[2] In this way, the enthalpic requirements of the system can be satisfied without as much of an entropic penalty.

5.E. Transition Enthalpies and Entropies. We can integrate the endothermic area in the scanning calorimetric heat flow from 120 to 160 °C to extract an enthalpy change for the transformation. The resulting value is 0.5 ± 0.1 kJ/(mol SiO_2) or 2.4 ± 0.3 kJ/(mol surfactant). The real question is how to interpret these values. The silica strain arguments presented above predict an endothermic transition because the lamellar phase appears to be an energetically less stable (more strained) state. Silica

strain in the composite is reduced from 140 to 160 °C, however, and thus, we expect the second step of the phase transformation (Figure 5) to be more endothermic than the first. By integrating the two peaks separately, we find transformation enthalpies of 0.4 ± 0.1 kJ/(mol SiO_2) for the 120−140 °C endotherm and 0.7 ± 0.1 kJ/(mol SiO_2) for the 140−160 °C endotherm, supporting our ideas about strain. Within this construction, our data agrees well with enthalpy differences measured between various porous silicas including calcined hexagonal surfactant templated silicas and pure silica zeolites.[50,51] Different pore size mesoporous silicas have enthalpy differences of 0.2−0.4 kJ/(mol SiO_2), whereas different zeolites have enthalpy differences ranging from 0.1 to 6.8 kJ/(mol SiO_2). The second step value of 0.7 ± 0.1 kJ/(mol SiO_2) is outside of the range observed for most mesoporous silicas but nicely in the range for different zeolitic structures, suggesting perhaps that some zeolites and the hexagonal composites that transform between 140 and 160 °C have more relaxed frameworks. Our overall enthalpy change from transformation could also be outside the energy range observed for different pore sized hexagonal silicas because, instead of changing the pore size, we are fully rearranging the organic domains and the framework to form layers.

If we assume the transformation occurs near equilibrium, we can also extract an entropy change from our enthalpy. The hexagonal-to-lamellar transformation has an entropy change of 1 J K^{-1} (mol SiO_2)$^{-1}$. This may be a slight underestimate if the equilibrium transformation takes place at somewhat lower temperature. This entropy change agrees well with the small third law entropy differences observed between various all silica zeolites.[52]

Because increased thermal disorder in the surfactant tails appears to drive the transformation, however, it is likely that part of the enthalpy and entropy change of the transition is associated with this organic conformational change. To put the enthalpy change in perspective, we can compare our measured value of 2.4 ± 0.3 kJ/(mol surfactant) with the enthalpy change of 1.3−1.4 kJ/(mol surfactant) for a hexagonal-to-lamellar phase transition (through an intermediate cubic phase) in a lyotropic liquid crystal.[53] The larger enthalpy change in a silica/surfactant composite probably results from the extra energy necessary to restructure the silica framework in addition to the organic domains, as discussed above. The calculated entropy of transformation for the composite is 6 J K^{-1} (mol surfactant)$^{-1}$, which is larger than the entropy change of 4.4−4.7 J K^{-1} (mol surfactant)$^{-1}$ for a hexagonal-to-lamellar phase transition (through an intermediate cubic phase) in a liquid crystal. Once again, this reinforces the idea that both the inorganic and the organic phase contribute significantly to the phase transformation energetics in silica/surfactant composites, with neither term being dominant.

The data collected on boric acid treated samples from 110 to 160 °C are much easier to interpret than the data for the water-treated sample because no phase change occurs. From 110 to 160 °C, there is also a negligible change in silica Q^4/Q^3 peak area ratio and only a small change in surfactant lost to solution (Figure 3, bottom, and Figure 6, bottom). Thus, the scanning calorimetric heat flow is generally flat.

6. Scanning Calorimetric Heat Flow from 160 to 190 °C. At 160 °C, scanning calorimetric heat flow curves from both water and boric acid treated samples overlap (Figure 2). As the temperature increases, data obtained on water-treated samples is endothermic, whereas data obtained on boric acid treated samples is exothermic. We note that, although data in this temperature range is more susceptible to drift than lower temperature data, the gross trends are fairly robust.

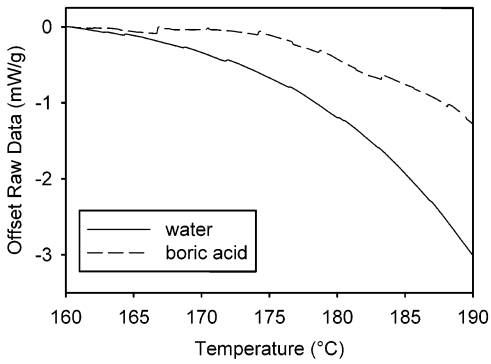

Figure 9. Raw (not background-subtracted) scanning calorimetric heat flow for a silica/surfactant composite hydrothermally heated in water (solid line) or in a boric acid buffer (dashed line) at 0.25 °C/min. To account for constant background offsets, the data is set to 0 at 160 °C. Treatment of a sample in water, where a lamellar phase is present, leads to a much larger endothermic signal then when a hexagonal phase is heated in a boric acid buffer. The endotherm is associated with entropy-driven conformational disordering of the surfactant tails. More tail motion is possible in the unconfined lamellar phase compared to the spatially confined hexagonal structure.

Above 160 °C in a boric acid treated sample, the framework polymerization increases and there is a corresponding exothermic region in the data. In addition, the amount of organic in solution mirrors the polymerization data (Figure 6, bottom) as both increase with increasing temperature. Surfactant degradation also occurs from 160 to 190 °C. Figure 7 (middle trace) shows that, by 190 °C, there are very small amine peaks corresponding to ∼3% of the organic in a boric acid treated composite. Although most of the exothermic signal in the region above 160 °C likely results from silica condensation, it could also result in part from a small amount of surfactant degradation and dimethyleicosylamine reincorporation into the organic domains.

Above 160 °C, the same chemical trends found in boric acid data are present in the water-treated sample: both condensation and surfactant degradation occur. However, an endothermic signal is observed for samples treated in water. To understand this, we need to remember that the boric acid and water-treated samples have different structural periodicities above 160 °C. The boric acid sample has a hexagonal geometry that confines the organic domains, whereas the water-treated sample has a layered structure that can expand freely. The lamellar structure is thus able to accommodate thermal disordering of the surfactant tails in a way that is not possible for a hexagonal composite. Unfortunately, our method of background subtraction using a second heating run could interfere with calorimetric signals caused by reversible expansion of the composite because these processes can also occur on the second run.

To explore the real difference between the water and boric acid treated samples, we thus plot the raw (not background subtracted) scanning calorimetric heat flow curves that have been offset to 0 mW/g at 160 °C (Figure 9). These curves are referenced only to pure water or pure boric acid buffer. In this case, both of the water and boric acid heat flow curves show endothermic behavior, consistent with entropy driven tail disordering. However, the water heat flow curve is much more endothermic than the boric acid heat flow curve. This may indicate that the nonconfined lamellar geometry allows more thermal disordering of the surfactant tails because interlayer swelling can easily accommodate the volume increase. In agreement with this idea, XRD data show that the water-treated sample swells at a rate of 0.68 Å/°C in the temperature range around 180 °C. The boric acid treated samples swell at only

0.21 Å/°C in this same temperature range. The different amount of swelling of the interlayer distances in hexagonal and lamellar mesophases may account for the difference in high-temperature calorimetric signals.

Conclusions

We have shown that scanning microcalorimetry can be used to explore the important energetic processes that occur during a phase transformation in inorganic/organic composite materials. For example, a previously unknown melting transition of the surfactant tails occurs at 70−71 °C. Thus, to hydrothermally restructure these composites, it is probably necessary to treat them above 70 °C where significant surfactant reorganization can occur. Silica condensation, by contrast, occurs during the whole heating ramp below 90 °C, regardless of surfactant tail mobility. It thus appears possible to tune the relative contributions of silica condensation and surfactant motion. To simply condense the framework in silica/surfactant composites, the sample should be hydrothermally heated at low temperature. To both condense the silica framework and restructure the composite, hydrothermal heating above 70 °C is necessary.

Two large endotherms between 110 and 160 °C in the scanning calorimetric heat flow for a sample hydrothermally heated in water are associated with the hexagonal-to-lamellar phase transformation. The presence of two clear peaks in the calorimetry allows us to conclude that the transformation proceeds in two steps. We postulate that the transition first occurs from a strained state at lower temperature and from a more relaxed state at higher temperature. Integration of the two endothermic transition peaks allows us to calculate an enthalpy change of $+0.5 \pm 0.1$ kJ/(mol SiO_2) or $+2.4 \pm 0.3$ kJ/(mol surfactant) for the hexagonal-to-lamellar phase transition. This endothermic value indicates that the transformation is entropically driven, likely stemming from increased conformation disorder of the surfactant tails in the lamellar phase. In addition, the positive value indicates that the hexagonal phase is stable with respect to the lamellar phase in the as-synthesized composites. The overall transition enthalpy is quite small, however, suggesting that entropic effects play a dominant role in determining structure in these inorganic/organic composite materials.

Acknowledgment. The authors thank Dr. L. Rene Corrales for sharing the calculated strain dependent activation energies and enthalpies of silica dissolution used in this work. This work was supported by the National Science Foundation under Grants DMR-9807190 (S.H.T.) and DMR-0101391 (A.N.) and by the Beckman Young Investigator program. This work made use of equipment supported by the National Science Foundation under Grant DMR-9975975. S.H.T. is an Alfred P. Sloan Foundation Research Fellow.

References and Notes

(1) Kresge, C. T.; Leonowitz, M. E.; Roth, W. J.; Vartuli, J. C.; Beck, J. S. *Nature* **1992**, *359*, 710. Beck, J. S.; Vartuli, J. C.; Roth, W. J.; Leonowicz, M. E.; Kresge, C. T.; Schmitt, K. T.; Chu, C. T.-W.; Olson, D. H.; Sheppard, E. W.; McCullen, S. B.; Higgins, J. B.; Schlenker, J. L. *J. Am. Chem. Soc.* **1992**, *114*, 10834.

(2) Huo, Q.; Margolese, D. I.; Stucky, G. D. *Chem. Mater.* **1996**, *8*, 1147.

(3) Gallis, K. W.; Landry, C. C. *Chem. Mater.* **1997**, *9*, 2035.

(4) Tolbert, S. H.; Landry, C. C.; Stucky, G. D.; Chmelka, B. F.; Norby, P.; Hanson, J. C.; Monnier, A. *Chem. Mater.* **2001**, *13*, 2247.

(5) Landry, C. C.; Tolbert, S. H.; Gallis, K. W.; Monnier, A.; Stucky, G. D.; Norby, P.; Hanson, J. C. *Chem. Mater.* **2001**, *13*, 1600.

(6) Gross, A. F.; Le, V. H.; Kirsch, B. L.; Tolbert, S. H. *Langmuir* **2001**, *17*, 3496.

(7) Xu, J.; Luan, Z. H.; He, H. Y.; Zhou, W.-Z.; Kevan, L. *Chem. Mater.* **1998**, *10*, 3690.

(8) Pevzner, S.; Regev, O. *Microporous Mesoporous Mater.* **2000**, *38*, 3:413.

(9) Zhao, D.; Huo, Q.; Feng, J.; Kim, J.; Han, Y.; Stucky, G. D.*Chem. Mater.* **1999**, *11*, 2668.

(10) Gross, A. F.; Ruiz, E. J.; Tolbert, S. H. *J. Phys. Chem. B* **2000**, *104*, 5448.

(11) Gross, A. F.; Le, V. H.; Kirsch, B. L.; Tolbert, S. H. *J. Am. Chem. Soc.* **2002**, *124*, 3713.

(12) Iler, R. K. *The Chemistry of Silica: Solubility, Polymerization, Colloid and Surface Properties, and Biochemistry*; Wiley: New York, 1979.

(13) Yang, S.; Navrotsky, A.; Phillips, B. L. *J. Phys. Chem. B* **2000**, *104*, 6071.

(14) Yang, S.; Navrotsky, A.; Phillips, B. L. *Microporous Mesoporous Mater.* **2001**, *46*, 137.

(15) Yang, S.; Navrotsky, A.; Phillips, B. L. *Microporous Mesoporous Mater.* **2002**, *52*, 93.

(16) Petrova, N.; Kirov, G. N. *Thermochim. Acta* **1995**, *269/270*, 443.

(17) Yang, S.; Navrotsky, A *Chem. Mater.* **2002**, *14*, 2803.

(18) Fournier, R. O.; Rowe, J. J. *Am. Mineral.* **1977**, *62*, 1052.

(19) Pereira, J. C. G.; Catlow, C. R. A.; Price, G. D. *Chem. Commun.* **1998**, 1387.

(20) Gross, A. F.; Le, V. H.; Kirsch, B. L.; Riley, A. E.; Tolbert, S. H. *Chem Mater.* **2001**, *13*, 3571.

(21) Impéror-Clerc, M.; Davidson, P.; Davidson, A. *J. Am. Chem. Soc.* **2000**, *122*, 11925

(22) Edler, K. J.; Reynolds, P. A.; White, J. W.; Cookson, D. *J. Chem. Soc., Faraday Trans.* **1997**, *93*, 199.

(23) Lindén, M.; Blanchard, J.; Schacht, S.; Schunk, S. A.; Schüth, F. *Chem. Mater.* **1999**, *11*, 3002.

(24) Schacht, S.; Janicke, M.; Schüth, F. *Microporous Mesoporous Mater.* **1998**, *22*, 485.

(25) Lapeña, A. M.; Gross, A. F.; Tolbert, S. H. Manuscript in preparation.

(26) Israelachvili, J. N. *Intermolecular and Surface Forces*, 2nd ed.; Academic Press: London, 1992.

(27) Blandamer, M. J.; Briggs, B.; Brown, H. R.; Burgess, J.; Butt, M. D.; Cullis, P. M.; Engberts, J. B. F. N. *J. Chem. Soc., Faraday Trans.* **1992**, *88*, 979. Blandamer, M. J.; Briggs, B.; Butt, M. D.; Cullis, P. M.; Gorse, L.; Engberts, J. B. F. N. *J. Chem. Soc., Faraday Trans.* **1992**, *88*, 2871.

(28) Kruk, M.; Jaroniec, M.; Sayari, A. *J. Phys. Chem. B* **1999**, *103*, 4590.

(29) Sayari, A.; Kruk, M.; Jaroniec, M.; Moudrakovski, I. L. *Adv. Mater.* **1998**, *10*, 1376.

(30) Corma, A.; Kan, Q.; Navarro, M. T.; Perez-Pariente, J.; Rey, F.*Chem. Mater.* **1997**, *9*, 2123.

(31) Kruk, M.; Jaroniec, M.; Sayari, A. *Microporous Mesoporous Mater.* **2000**, *35*−*36*, 545.

(32) Sayari, A. *Angew. Chem., Int. Ed.* **2000**, *39*, 2920.

(33) Sitkoff, D.; Ben-Tal, N.; Honig, B. *J. Phys. Chem.* **1996**, *100*, 2744.

(34) Cabani, S.; Gianni, P.; Mollica, V.; Lepori, L. *J. Soln. Chem.* **1981**, *10*, 563.

(35) Norby, P. *J. Am. Chem. Soc.* **1997**, *101*, 55215. Norby, P.; Hanson, J. C. *Catal. Today* **1998**, 39, 301.

(36) Muntean, J. V.; Stock, L. M.; Botto, R. E. *J. Magn. Reson.* **1988**, *76*, 540.

(37) Because this experiment makes use of a constant volume calorimeter, we are technically measuring changes in internal energy of the entire system, rather than enthalpy. Because all processes with significant calorimetric signatures take place in the condensed phase, however, the pressure and volume terms are negligible, and thus, there is almost no difference between enthalpy and internal energy. Moreover, because there is a vapor space in the calorimeter, the liquid volume is not fixed. Within the error in the values, we thus feel that it is quite safe to report integrations of the scanning calorimetry heat flow as enthalpies.

(38) Bunn, A.; Cudby, M. E. A.; Harris, R. K.; Packer, K. J.; Say, B. J. *Polymer* **1982**, *23*, 694.

(39) Simmonutti, R.; Comotti, A.; Bracco, S.; Sozzani, P. *Chem. Mater.* **2001**, *13*, 771.

(40) Wang, L.-Q.; Liu, J.; Exarhos, G. J.; Bunker, B. C. *Langmuir* **1996**, *12*, 2663.

(41) Takegoshi, K.; Hikichi, K. *J. Chem. Phys.* **1991**, *94*, 3200.

(42) Van Ginhoven, R. M., PhD Thesis, University of Washington, 2002.

(43) Private communication with L. Rene Corrales, thesis advisor for endnote 42.

(44) Gladden, L. F.; Carpenter, T. A.; Elliott, S. R. *Philos. Mag. B* **1986**, *53*, L81.

(45) Mentzen, B. N.; Letoffe, J.-M.; Claudy. P *Thermochim. Acta* **1996**, *288*, 1.

(46) Topor, L.; Navrotsky, A.; Zhao, Y.; Weidner, D. J. *J. Solid State Chem.* **1997**, *132*, 131.

(47) Yashima, M.; Mitsuhashi, T.; Takashina, H.; Kakihana, M.; Ikegami, T.; Yoshimura, M. *J. Am. Ceram. Soc.* **1995**, *78*, 2225.
(48) Linde, R. K. *J. Phys. Chem.* **1965**, *69*, 4407.
(49) Gallis, K. W.; Landry, C. C. *Chem. Mater.* **1997**, *9*, 2035.
(50) Navrotsky, A.; Petrovic, I.; Hu, Y.; Chen, C.-Y.; Davis, M. E. *Microporous Mater.* **1995**, *4*, 95.
(51) Piccione, P. M.; Laberty, C.; Yang, S.; Camblor, M. A.; Navrotsky, A.; Davis, M. E. *J. Phys. Chem. B* **2000**, *104*, 10001.
(52) Piccione, P. M.; Woodfield, B. F.; Boerio-Goates, J.; Navrotsky, A.; Davis, M. E. *J. Phys. Chem. B* **2001**, *105*, 6025.
(53) Nishizawa, M.; Saito, K.; Sorai, M *J. Phys. Chem. B* **2001**, *105*, 2987.